Journal of New Materials for Electrochemical Systems 15, 151-156 (2012)

DFT Study of the CO Poisoning Effects on Pd_xCu_{1-x} (110) Surface

Ernesto López-Chávez[1,*], Alberto García-Quiroz[1], Yesica A. Peña-Castañeda[1], Fray de Landa Castillo-Alvarado[2], Gerardo Cabañas-Moreno[3] and José Manuel Martínez-Magadán[4]

[1]Universidad Autónoma de la Ciudad de México. Av Fray Servando Teresa de Mier #92, Col Centro, CP 06080, Mexico D.F., Mexico
[2]Instituto Politécnico Nacional, Edificio 9, ESFM - UPALM, Col. Lindavista, Mexico D.F., CP 07738, Mexico
[3]Instituto Politécnico Nacional. Centro de Nanociencias y Micro y Nanotecnología - UPALM, Col. Lindavista, Mexico D.F., CP 07738, Mexico
[4]Instituto Mexicano del Petróleo, Eje Central Lázaro Cárdenas Norte #152, Col. San Bartolo Atepehuacán, CP 07730, Mexico D.F., Mexico

Received: November 30, 2011, Accepted: February 07, 2012, Available online: April, 10, 2012

Abstract: *CO contaminants play a significant role in modifying the performance of proton exchange membrane fuel cells (PEMFC). Pt is probably the most common catalyst being used today to absorb CO in the PEMFC, yet recent studies have shown that the use of Pd alloys such as Pd-Cu can increase the fuel cell efficiency versus a pure Pt catalyst. In this work, we examine the adsorption of CO onto Pd_xCu_{1-x} (110) surfaces, with different values of x, in order to improve the CO tolerance. Understanding how molecules interact with such surfaces is the first step in understanding catalytic reactions. The study here presented was done using CASTEP, a computational code based on the plane-wave pseudopotential method of functional density theory. The surface structure of Pd_xCu_{1-x} (110) was optimized and then the state density-functional, the repulsion energies and the chemisorption for CO on Pd_xCu_{1-x}(110) were calculated. The results indicate that chemisorption energies of CO on Pd_xCu_{1-x} are highly dependent on the concentration x of the alloy. In addition, density of states analysis indicate that the poisoning effect is partially due to the loss of Pd-Cu(d) electrons upon CO adsorption.*

Keywords: catalysts, CO poisoning, PEMF cell, molecular simulation, DFT Theory

1. INTRODUCTION

Proton exchange membrane fuel cells (PEMFCs), which convert with great efficiency the chemical energy of a fuel directly into electricity, are one of the key technologies for the generation of clean and sustainable energy [1-3], a pressing need of the 21st century. Still, some technological challenges are yet to be solved in order to achieve complete commercialization. Among them, the development of electrocatalysts tolerant to CO at levels of 50 ppm (with a noble metal loading of 0.1 mg cm^{-2} or less) is deemed to be one of the most significant barriers that PEMFCs must overcome [4]. Carbon monoxide, which commonly exists in fuel gas, has long been recognized as a source of poison to Pt-based anodes, widely used for their outstanding catalytic reactivity toward hydrogen dissociation and oxidation [5,6]. The net result is a diminished efficiency of the cell. The poisoning effect is especially significant at the relatively low temperatures at which PEMFCs operate [7]. Indeed, actual membrane- electrode assemblies (MEAs) cannot tolerate such high CO levels at the current PEMFC stack operating temperatures (around 80°C).

Although a great deal of effort has been put into the exploration of cost-effective, active, and stable fuel cell catalysts, there have not been yet any real breakthroughs. Exploring new catalysts, improving catalyst activity and stability/durability, and reducing catalyst cost are currently the major tasks in the development of a cost efficient fuel cell technology. In the search for alternative low-cost non-Pt catalysts, researchers have looked in diverse directions, including supported platinum group metal (PGM) types such as Pd-, Ru-, and Ir-based catalysts, bimetallic alloy catalysts, transition metal macrocycles, and transition metal chalcogenides

*To whom correspondence should be addressed: Email: elopezc_h@hotmail.com
Phone:

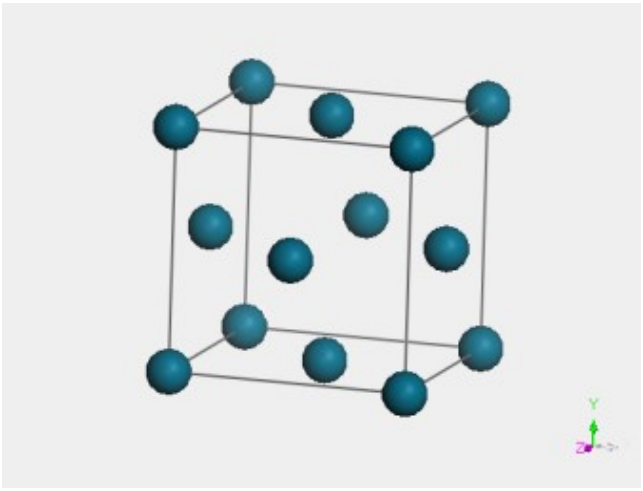

Figure 1. Typical PdCu bi-metal molecule on a FCC structure constructed and geometry optimized.

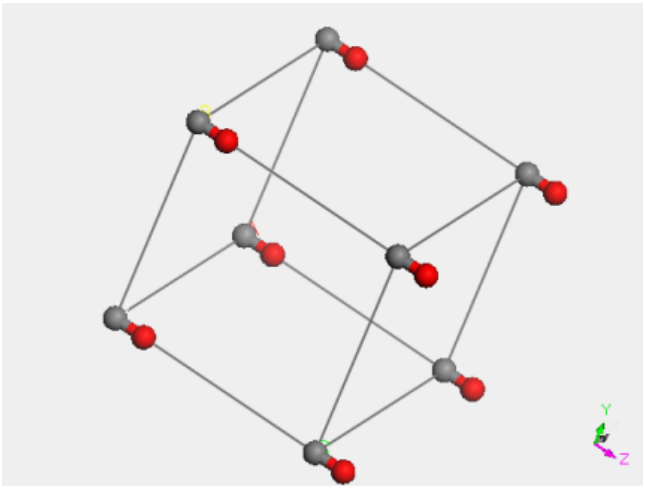

Figure 2. Typical CO molecule into a CC structure constructed and geometry optimized.

[8,9,10] among others.

More specifically, Pd [11] or Ru [12] have been used as catalysts for the preferential oxidation of CO at low temperature. The Ru catalyst has exhibited high performance for preferential oxidation of CO and long-term stability under a low O2/CO molar ratio. However, as considerable amounts of precious metals are used in the shift converter unit as well as in the CO preferential oxidation unit, the use of Ru results in a higher cost. Moreover, this complicated system containing a CO removal unit reduces both efficiency and reliability.

In this work, we study Pd_xCu_{1-x} binary alloy surfaces in order to find an anode less expensive than pure Pt for polymer electrolyte membrane fuel cells (PEMFC), while minimizing the poisoning by CO in the catalyst. As there is information that leads us to believe that the replacement of Pt by Pd would decrease the cost by a factor of 5 [13, 14], we have explored possible alloys [15, 16] of Pd that might lead to higher performance.

Most theoretical studies on the effect of CO poisoning on the catalyst use clusters of atoms to simulate the catalyst surface, and do not take into account its crystal structure. In this work, we use alternative method. First, we built a bulk alloy of *Pd-Cu* with fcc structure, and a modeled compositional disorder within the crystal. Disorder was described in terms of a hybrid atom (pseudo-atom) put in atomic sites of the crystal lattice, in what is called a mixture atom description. The *x* concentration was then used to simulate the case where one atomic site is randomly occupied by two or more different types of atom. In the case of the alloy Pd_xCu_{1-x}, x represents the probability that the site studied is occupied by the atom *Pd.* This method allows the creation of mixtures of different elements, leading to a mixture of *Pd* and *Cu* properties.

Experimentally, Pope, Griffiths and Norton [17] have studied the catalyst surface structures. They formed the alloy structures by the deposition of 0–4 monolayers (ML) of Pd on Cu(100) at 300 K. c(2 × 2) surface alloy and p4g interfacial alloy structures are seen at 0.5 and 1.0 ML Pd coverages, respectively. Pope results showed that valence band spectra resemble those of dilute Pd-Cu bulk alloys below 0.5 ML Pd coverage. At higher coverages they become increasingly Pd-like. The Pd (Cu) core level binding energies increase (decrease) in the alloys. CO chemisorption on Pd sites is weakened relative to Pd(100), but the desorption temperature of CO from Cu does not change. For CO adsorption on Cu(100) they showed that the sticking coefficient decreases significantly with CO coverage, even below 0.5 ML. The additional CO adsorbed on formation of the compressed overlayer fills a low-temperature desorption state.

In the present theoretical study it is shown that the chemisorption energies of CO on Pd_xCu_{1-x} are highly depend on the concentration of the alloy, and that the catalyst poisoning arises from the loss of Pd_xCu_{1-x} (d) electrons upon CO adsorption. From now on we are going to use Pd_xCu_{1-x} as the $Pd_{100\%-y}Cu_y$ notation in a discretional way.

2. METHODOLOGY AND COMPUTATIONAL DETAILS

Our goal was to construct a theoretical bi-metal $Pd_{100\%-y}Cu_y$ molecule interacting with carbon monoxide gas-molecules. In order to qualify catalytic poisoning on copper palladium metal to that gas we constructed $Pd_{100\%-y}Cu_y$ (110) theoretical surfaces as well as the correspondent (1 × 1) and (2 × 1) surfaces. The y-value ranged from 0% to 10% of copper metal considering 2% variation concentrations. To construct the disordered alloy we used the virtual crystal approximation [18] of the mixture atom description. The quantum mechanical calculations described here are based on density functional theory (DFT) [19-24]. The gradient-based BFGS minimization [25] algorithm was used for the task of optimizing the geometry.

The surface calculations were realized using CASTEP of Materials Studio [19], starting from the optimized structure from the Pd_xCu_{1-x} bulk part. Next, we cleaved the bulk in order to obtain the surface (110), thus opening a new 2D periodic surface. After that a vacuum slab was built. Then, the structure was changed from 2D to 3D periodic, and a vacuum was added above the atoms to input the system anew in CASTEP.

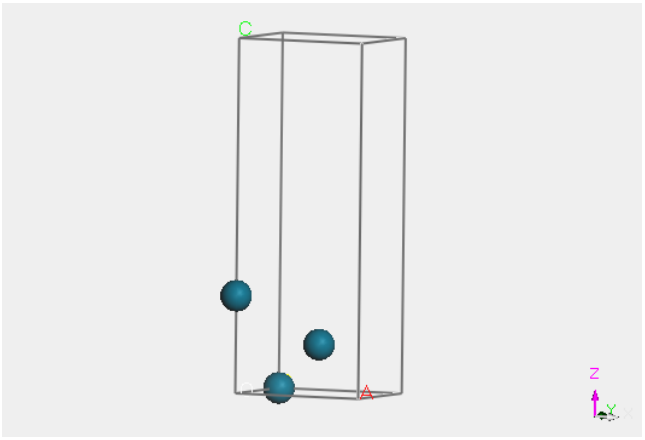

Figure 3. Typical PdCu (110) surface in a crystalline structure, geometry optimized in the absence of CO.

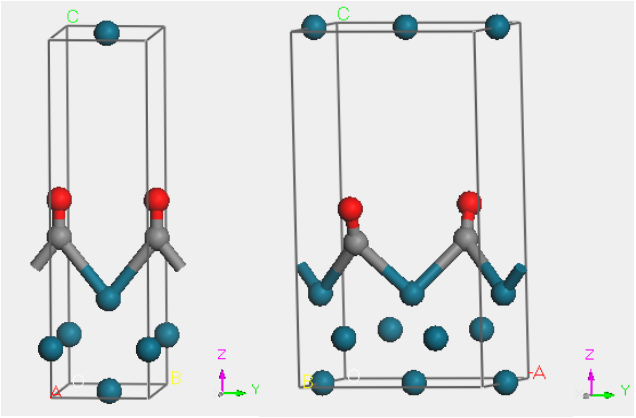

Figure 4. Left: Typical (1 x 1) CO on PdCu (110) surface in a crystalline structure with optimized geometry. Right: (2 x 1) CO on PdCu (110) surface in a crystalline structure with optimized geometry.

The BFGS scheme uses a starting Hessian which is recursively updated during optimization. The CASTEP implementation involves a Hessian in the mixed space of internal and cell degrees of freedom, so that both lattice parameters and atomic coordinates can be optimized. For exchange-correlation effects, we used the "generalized gradient approximation" in the form suggested by Perdew, Burke and Ernzerhof, GGA-PBE [26, 27].

To build and optimize every $Pd_{100\%-y}Cu_y$ bi-metal bulk and the carbon monoxide molecules we used primitive cell optimization and an energy optimization of the geometry. Fig. 1 shows this first step in a face centered cell (FCC).

In order to carry out the geometry optimization of the CO molecules we had to insert them into a simple cubic crystal (CC) lattice. With the use of the modeling software, a C-O bond length value of 1.1539 Å was found for the CO molecule, similar to the 1.12 Å experimental value found in literature (Fig. 2).

The next step was to build $Pd_{100\%-y}Cu_y$ (110) surfaces. The $Pd_{100\%-y}Cu_y$ (110) surfaces were relaxed and optimized selecting a

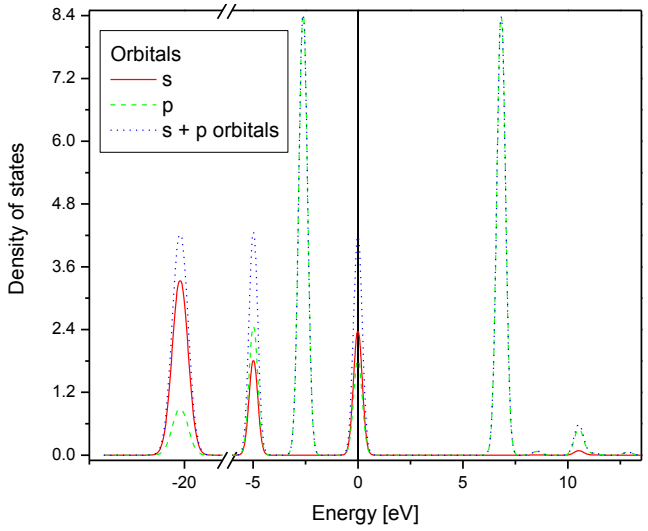

Figure 5. Density of states of CO molecule into crystal.

k-points parameters field as 3x4x1 in order to calculate the Density of States (DOS) for these systems (Fig. 3).

After that, CO molecules where added to the $Pd_{100\%-y}Cu_y$ (110) surfaces and geometry was again optimized. These surfaces allowed us to get the (1 x 1) CO on $Pd_{100\%-y}Cu_y$ (110) and the (2 x 1) CO on $Pd_{100\%-y}Cu_y$ (110) surfaces. The energies and the density of states (DOS) of each of the crystalline structures was then analyzed after yet another optimization of geometry (Fig. 4[left] and Fig. 4[right]).

A supercell modeling software tool was used to change from the 1 x 1 to the 2 × 1 $Pd_{100\%-y}Cu_y$ (110) surfaces. For this structure the k-points parameters had to be modified to 2x3x1 on the geometry optimization analysis. Chemisorption and repulsion energies were calculated using the previously described results.

The average chemisorption energy of CO on Pd-Cu(110) binary alloy surfaces was evaluated using the following equation:

$$\Delta E_{chem} = 0.5E_{(2\times1)Pd_xCu_{1-x}(110)} - E_{Pd_xCu_{1-x}(110)} - E_{CO_{molecules}} \quad (1)$$

While for the repulsion energy we considered:

$$\Delta E_{rep} = 0.5E_{(2\times1)Pd_xCu_{1-x}(110)} - E_{Pd_xCu_{1-x}(110)} \quad (2)$$

At last we examined the changes in the density of states (DOS,) which gave us an insight into the bonding mechanism of CO on $Pd_{100\%-y}Cu_y$ (110).

3. RESULTS AND DISCUSSION

The effect of poisoning on various catalyst structures has been object of a wide range of theoretical studies, using both empirical and first-principle methods. Most of these consider clusters of atoms of a candidate catalyst for CO adsorption. Four possible adsorption modes have been investigated: the on-top site (O), the 2-fold edge (E), the 3-fold hollow site (H), and the side-on configuration on the edge (L). In these studies the H and L modes were found to be unstable upon full geometry optimizations. In both cases, the CO molecule migrates to the on-top site [28]. In the pre-

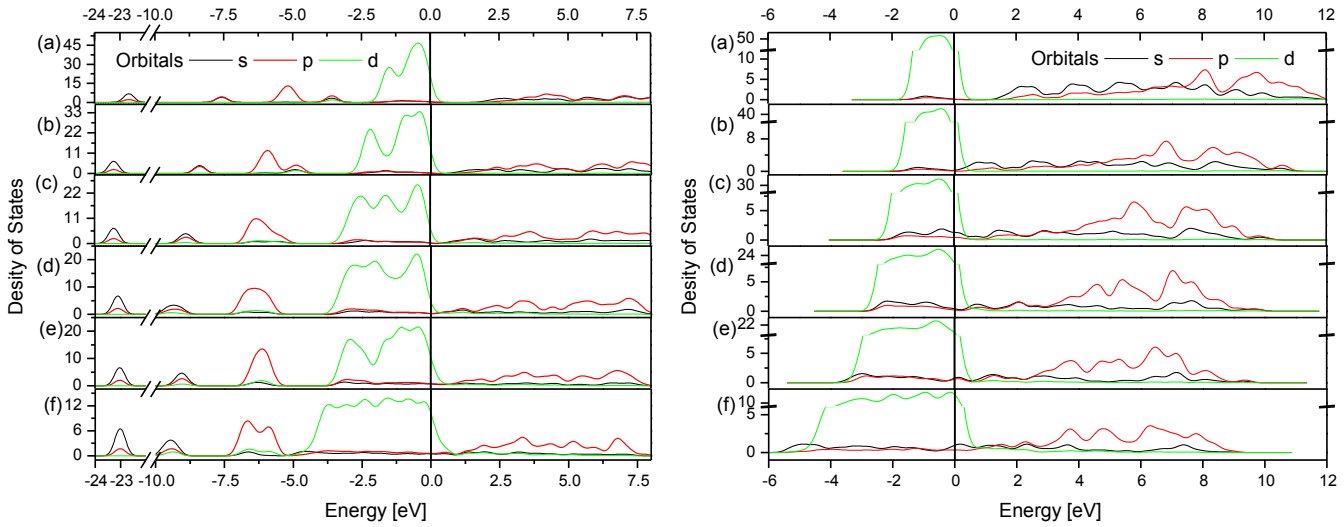

Figure 6. a)[left] $Pd_{0.9}Cu_{0.1}$(110) (2x1) surface interacting with CO molecules, a)[right] and $Pd_{0.9}Cu_{0.1}$(110) (2x1) surface density of states respectively. b)[left] $Pd_{0.92}Cu_{0.08}$(110) (2x1) surface interacting with CO molecules, b)[right] $Pd_{0.92}Cu_{0.08}$(110) (2x1) surface density of states respectively. c)[left] $Pd_{0.94}Cu_{0.06}$(110) (2x1) surface interacting with CO molecules, c)[right] $Pd_{0.94}Cu_{0.06}$(110) (2x1) surface density of states respectively. d)[left] $Pd_{0.96}Cu_{0.04}$(110) (2x1) surface interacting with CO molecules, d)[right] $Pd_{0.96}Cu_{0.04}$(110) (2x1) surface density of states respectively. e)[left] $Pd_{0.98}Cu_{0.02}$(110) (2x1) surface interacting with CO molecules, e)[right] $Pd_{0.98}Cu_{0.02}$(110) (2x1) surface density of states respectively. f)[left] $Pd_{1.0}$(110) (2x1) surface interacting with CO molecules, f)[right] $Pd_{1.0}$(110) (2x1) surface density of states respectively.

sent study, we attempt to model the chemistry of CO-poisoning on catalyst by means of interactions between CO with surfaces of Pd_xCu_{1-x}(110). The coverage of CO used in these calculations was of 0.50 ML. The binary alloy surface provides a useful representation of the active on-top site, deemed to be essential in many realistic catalytic reactions. The CO molecules were placed on the on-top sites on surfaces of Pd_xCu_{1-x}(110), as shown in Fig. 4. The surfaces structure of Pd_xCu_{1-x}(110) remains nearly intact upon structural relaxation.

Fig. 5 displays the calculated projected density of states (PDOS) of the CO-molecule, while Fig. 6 shows the bare Pd_xCu_{1-x}(110) surfaces and the CO-poisoned Pd_xCu_{1-x}(110) surfaces, with x=1.0, 0.98, 0.96, 0.94, 0.92, 0.90. The band structure of isolated CO presents four bands below the Fermi level: three bands filled with s- and p-electrons, centered on the energies 0, -5.0 eV and -20 eV, and a p-band, which is centered on the energy -2.5 eV. For x=0.98, 0.96 and 0.94 (Fig. 6[c-e], the band structure of (2x1) Pd_xCu_{1-x} (110) has, in the absence of CO, a single-band below the Fermi level, which is occupied by d-, s-, p-electrons. As the Cu concentration increases, the bands of the Pd-Cu surface are elevated, still in the absence of CO, from 27 electrons/eV to 55 electrons/eV. These bands are filled mostly with d-electrons. In these figures we see that the occupied lowest energy in this band increases from -3.5 eV to -1.8 eV as the concentration x decreases. This means that Cu transfers more d-electrons to the band of the alloy, and as a side effect the band is shifted to energies near the Fermi level, so that at greater Cu concentrations the alloy will have it easier to transfer electrons to the band structure of CO, thereby reducing chemisorption energy (see table 1).

Table 1. Energies of chemisorption and repulsion in function of the Cu concentration

Pd_xCu_{1-x} alloys	Chemisorption energy (eV)	Repulsion energy (eV)
x=0.90	0.061	-0.079
x=0.92	-0.305	-0.163
x=0.94	-0.807	-0.326
x=0.96	-1.202	-0.450
x=0.98	-1.313	-0.053
x=1.00	-1.627	-0.064

Experimental results indicate that at low coverage of CO (0.5 ML), CO prefers to bind to top sites while our DFT calculations consistently predict that CO prefers adsorption at hollow sites, however, the results showed in table 1 indicated that the energies of chemisorptions and repulsion, for coverage of CO used in these calculations (0.5 ML), are in good agreement with experimental results. The discrepancy is generally attributed to the overestimation of the HOMO-LUMO gap of CO [17]. A number of theoretical methods have been proposed to correct this problem. Only very few theoretical studies have investigated the CO adsorption at high coverage.

Figures 5 through 7 indicate that in the presence of CO, the d-bands of (2x1) PdxCu1-x (110) below the Fermi level are enhanced, with CO loading on the binary alloy as the CO(σ) orbital donates electrons to the d-band. It is noted that, for concentrations of 0.98, 0.96 and 0.94, three additional bands of s-, p- and d-orbitals are formed below the Fermi level. While at concentrations

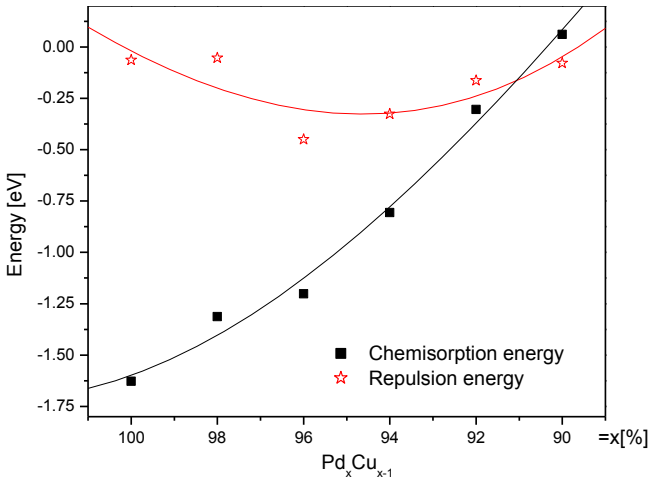

Figure 7. Behavior of the energies of chemisorption and repulsion (eV) of the CO molecule on the surface (110) of the Pd_xCu_{1-x} alloy in function concentration of Cu.

of 0.92 and 0.90 a fourth band of s-electrons is formed below the Fermi level. These results indicate that as the copper concentration increases, the s electrons of the first band and the p and d electrons of the third band move into an additional band centered around -4.5 eV.

As copper concentration increases, s- and p-electrons of the bands of CO and d-electrons of Pd-Cu band, nearest to the Fermi level, begin to form an additional band, which is centered around of -4.9 eV for x=0.92, and -3.5 eV for x=0.90. This mechanism also makes some of the d electrons available for exchange between CO and Pd-Cu, thereby reducing energy chemisorption. In parallel, the π^*-bands of CO molecules move downward roughly upon receiving back-donation of d-electrons from the Pd_xCu_{1-x}(110) surfaces.

Fig. 7 shows the behavior of the energies of chemisorption and repulsion of the CO molecule on the surface (110) of the Pd_xCu_{1-x} alloy. We observe that, as the concentration of Cu increases, the CO molecule binds to the surface with less intensity. This observation indicates that the increase of small amounts of Cu helps to reduce the effect of CO poisoning, which is in good agreement with some experimental data [29, 30].

Otherwise, based on the Hirshfeld charge analysis [31], the mechanism can be interpreted as that electron flow from Pd_xCu_{1-x} (d) to CO π^*-orbitals dominates the binding process and the surface (110) of the Pd-Cu alloy acts as an electron donor. The calculated electron loss per CO decreases monotonically as the Cu concentration increases. The electron back-donation from the d-band of the Pd-Cu alloy to the antibonding π^*-orbital of CO gives rise to a looser C-O bond and consequently the C-O bond length is elongated.

4. CONCLUSIONS

Catalyst poisoning by CO has been long recognized as one of the major obstacles to the progress and commercialization of the PEM fuel cells. In this work, we investigated part of the catalytic processes of poisoning of Pd_xCu_{1-x}(110) by CO by employing calculations based on density functional theory. Our results indicate that increasing amounts of Cu help to reduce the effect of CO poisoning, in good agreement with some experimental data.

In order to find the mechanism of poisoning it was necessary to obtain the density of the energy states of the Pd-Cu (110) surfaces with and without CO molecules. The mechanism can be interpreted as a result an electron flow from Pd_xCu_{1-x}(d) to CO π^*-orbitals dominating the binding process, the surface (110) of the Pd-Cu alloy acting as an electron donor. The calculated electron loss per CO decreases monotonically as the Cu concentration increases. The loss of Pd_xCu_{1-x}(110)(d) electrons as well as the physically blocked binding sites upon CO poisoning leads to a performance degradation of the Pd-Cu catalyst.

5. ACKNOWLEDGMENTS

Project supported by the Institute of Science and Technology of DF (ICYT-DF), under the agreement PIUTE10-32. We also acknowledge, for the partial finantial support, to Sistema Nacional de Investigadores from Consejo Nacional de Ciencia y Tecnología (Mexican government foundation), SNI-CONACyT and to the Universidad Autónoma de la Ciudad de México, UACM.

REFERENCES

[1] B.C.H. Steele, A Heinzel, Nature, 414, 345 (2001).
[2] R. Bashyam, P. Zelenay, Nature, 443, 63 (2006).
[3] F. Barbir. PEM fuel cells: theory and practice. New York: Elsevier Academic Press, 2005.
[4] R.G. Herman, K. Klier, G.W. Simmons, B.P. Finn, J.B. Bulko, T.P. Kobylinski, J. Catal. 56, 407 (1979).
[5] S. Alayoglu, A.U. Nilekar, M. Mavrikakis, B. Eichhorn, Nat. Mater. 7, 333 (2008).
[6] X. Cheng, Z. Shi, N. Glass, L. Zhang, J. Zhang, D. Song, Z. Liu, H. Wang, J.J. Shen, Power Sources, 165, 739 (2007).
[7] M.M. Gadgil, R. Sasikala, S.K. Kulshreshtha, J. Mol. Catal., 87 (1994).
[8] S. Ye, P. Beattie, S.A. Campbell, D.P. Wilkinson. Anode catalyst compositions for a voltage reversal tolerant fuel cell. US Patent Appl. 2004/0013935.
[9] T.R. Ralph, M.P. Hogarth, Platinum. Metals. Rev., 46, 117 (2002).
[10]S.D. Knights, K.M. Colbow, J. St-Pierre, D.P. Wilkinson. J. Power Sources, 127 (2002).
[11]R.L. Borup, J.R. Davey, F.H. Garzon, D.L. Wood, M.A Inbody, J. Power Sources, 163, 76 (2006).
[12]S. Ye, M. Hall, H. Cao, P. He, ECS Transactions 3,1, 657 (2006).
[13]Web page: www.kitco.com/market/.
[14]K. Kinoshita, Electrochemical Oxygen Technology, Wiley: New York, 1992.
[15]J.L. Fernandez, V. Raghuveer, A. Manthiram, A. Bard, J. Am. Chem. Soc. 127, 13100 (2005).
[16]A. Sarkar, A.V. Murugan, A. Manthiram, J. Mater. Chem. 19, 159 (2009).
[17]T.D. Pope, K. Griffiths, P.R. Norton, Surf. Sci, 306, 30 (1994).
[18]L. Bellaiche, D. Vanderbilt, Phys. Rev. B, 61, 7877 (2000).

[19]Web page: www.accelrys.com
[20]P. Hohenberg, W. Kohn, Phys. Rev. B, 136, 864 (1964).
[21]W. Kohn, L. Sham, J, Phys. Rev. A, 140, 1133 (1965).
[22]M. Levy in Proc. Natl. Acad. Sci. U. S. A., 76, 6062 (1979).
[23]R.G. Parr, W. Yang, Density-Functional Theory of Atoms and Molecules, Oxford University Press, Oxford, 1989.
[24]E.S. Krychko, E.V. Ludena. Energy Density Functional Theory of Many-Electron Systems, vol. 4 of Understanding Chemical Reactivity, Kluwer Academic Publishers, Dordrecht, 1990.
[25]B.G. Pfrommer, M. Cote, S.G. Louie, M.L. Cohen, J. Comput. Phys., 131, 133 (1997).
[26]J.P. Perdew, K. Burke, M. Ernzerhof, Phys. Rev. Lett., 77, 3865 (1996).
[27]X. Xu, W. Goddard III, J. Chem. Phys., 121, 9 (2004).
[28]L. Chen, B. Chen, CH. Zhou, R. Forrey, H.J. Cheng, J. Phys. Chem. C., 112, 1394 (2008).
[29]G.J. Blyholder, J. Phys. Chem., 68, 2772 (1964).
[30]X.Wang, N.N, Kariuki, S.M. Niyogi, D.J. Smith, T. Myers, Y. Hofmann, M. Zhang and C. Heske, 214th ECS Meeting, October 12–17, Honolulu, Hawaii, 2008.
[31]Y. Sha, T. Yu, B.V. Merinov, A. van Duin, and W.A. Goddard III, 214th ECS Meeting, October 12–17, Honolulu, Hawaii, 2008.